Surface Defect Detection Method of Composite Materials Based on Deep Learning

LU Yonghua[1*], *HUANG Yu*[1], *XU Jiajun*[1], *FENG Qiang*[2], *ZHOU Lihua*[2]

1. College of Mechanical & Electrical Engineering, Nanjing University of Aeronautics & Astronautics, Nanjing 210016, P. R. China;

2. State-Owned Jinjiang Machinery Factory, Chengdu 610043, P. R. China

(Received 5 December 2022; revised 31 May 2023; accepted 19 July 2023)

Abstract: With the development tendency of energy saving and weight reduction of aerospace materials, high-performance composite materials have been widely used in aircraft skins. However, the surface quality detections of composite skin parts are mostly carried out manually, leading to low detection efficiency and low accuracy. Visual detection has gained more and more attention in recent years, mainly because of its non-destructive detecting characteristics with high precision and flexibility. In view of the visual detection requirements of surface defects of composite skin parts, a robot-based detection platform was constructed, which innovatively integrated manipulator module, image acquisition module, laser ranging module, the deep learning module, and the complementary upper computer software. In order to ensure the efficiency and accuracy of detection, the detection algorithm of the system was developed based on YOLOv5. In addition, on account of the lack of raw composite skin parts, the dataset for training was expanded by employing the following three methods: Mirroring and rotating, translating, and adding noise. Experiments validate that the system can realize online, automatic, and accurate detections of various types of composite skin parts. The proposed system can complete detection of an image with a size of 5 496 pixel× 3 672 pixel in 0.744 s, and the detection accuracy reaches 96.35%, which meets the requirements for composite surface quality detection.

Key words: composite material skin; visual detection; YOLO; object detection; manipulator

CLC number: TP23 **Document code:** A **Article ID:** 1005-1120(2023)04-0487-13

0 Introduction

In recent years, aviation materials have been developing in the direction of light weight and high strength. Due to their excellent properties, carbon fiber composite materials are more and more widely used in aircraft skins. Structurally, the composite materials exhibit good strength along the fiber axis, which also accompanies the characteristics of high temperature resistance, corrosion resistance, high hardness, and high strength. It is precisely because of the increasing application of composite materials in aircraft skins, their quality detection has attracted much attention.

Foreign scholars have applied machine vision, infrared thermal imaging, ultrasonic detection and other technologies to aircraft skins detection. Carnegie Mellon University developed the skin detection robot ANDI (Automated non-destructive inspector), which drawn on bionics and used suction cups to crawl on the surface of the aircraft. The robot was equipped with four industrial cameras and an eddy current probe, which can be controlled remotely. The function of cameras is mainly to navigate the robot's motion and detect the surface defects of the aircraft skins. The eddy current probe used the phenomenon of electromagnetic induction to detect the dark seams and cracks that were difficult to find[1]. At present, the fourth-generation wall-climbing ro-

*Corresponding author, E-mail address: nuaa_lyh@nuaa.edu.cn.

How to cite this article: LU Yonghua, HUANG Yu, XU Jiajun, et al. Surface defect detection method of composite materials based on deep learning[J]. Transactions of Nanjing University of Aeronautics and Astronautics, 2023, 40(4): 487-499.

http://dx.doi.org/10.16356/j.1005-1120.2023.04.009

bot has been developed, equipped with more advanced detecting equipments, and has a high degree of automation, reliability and efficiency[2-3]. NASA's Propulsion Technology Laboratory researched and developed the multifunction automated crawling system (MACS) series of wall-climbing robots, which could be equipped with different equipments to move quickly on the surface of the aircraft to detect defects on the surface of the aircraft skins.

Due to the use of wired power supply, it cannot perform complete detection of the whole aircraft[4-5]. Domestic researches mainly focus on traditional image processing algorithms and deep learning algorithms. The traditional machine vision processing algorithms were used by Sheng[6] to extract the texture of the aircraft skins with the grayscale co-occurrence matrices, which achieved the detection of rusty rivets. Liu[7] completed the recognition of aircraft surface skin defects and types by using the visual detection technologies of deep neural network, which finally significantly improved the efficiency and accuracy of detection. Yan[8] combined support vector machines(SVMs) and machine learning to process infrared images of aircraft skins, and compared the recognition results of symplectic group algorithms and SVM classification algorithms.

It is very easy for the human eyes to find the targets of interest in the image, but the computer can only obtain the pixel values of 0—255 in the image, so it is difficult to find the precise position of the targets of interest in the image. As shown in Fig.1, the traditional object detection process generally includes three steps. The first step is region proposal. The purpose of region proposal is to find regions of interest (ROI) in the input image, which is the regions where objects may exist. Due to the different sizes and positions of the targets, most traditional methods apply sliding windows of different sizes to traverse the input image multiple times, thereby obtaining a large number of ROIs[6-8]. The second step is feature extraction. At present, many scholars have proposed some relatively mature feature extraction algorithms, such as histogram of oriented gradient (HOG)[9], scale invariant feature

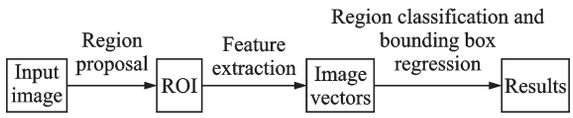

Fig.1 Steps of traditional object detection

(SIFT)[10], local binary pattern feature (LBP)[11], and so on. The third step is region classification and bounding box regression, which classifies the feature vectors in the regions of interest and outputs the target detection results.

With the development of deep learning technologies and computer hardwares, scholars have developed more and more efficient and high-precision target detection algorithms. Over-Feat[12] was a pioneer in combining deep learning with object detection, with the mean average precision (mAP) reached 24.3% on the ILSVRC2013 dataset. Shortly after Over-Feat was proposed, Girshick et al.[13] came up with the R-CNN model, and the detection effect was greatly improved compared with Over-Feat, which achieved 58.5% accuracy on the VOC2007 dataset. He et al.[14] proposed the SPP-Net algorithm, which introduced the spatial pyramid pooling (SPP) layer, and the average accuracy on the VOC2007 dataset reached 60.9%. Then the Fast R-CNN[15] model was put forward, which used VGG16 instead of AlexNet, and the mAP reached 70.0%. Compared with R-CNN, the training speed increased by 8.8 times, the detection speed increased by 213 times.

Liu et al.[16] proposed Steel-Yolov3, surface defect detection algorithm for shaped steel based on deformable convolution and multi-scale dense feature pyramid. The algorithm was used to detect defects such as scarring, peeling, scratches and injuries on the surface of section steel with a size of 104 pixel × 104 pixel, with an accuracy of 89.24% and the detection efficiency of 25.62 f/s. Tian et al.[17] proposed a steel surface defect detector, DCC-CenterNet. The experimental results show that on the NEU-DET steel defect dataset, the accuracy of DCC-CenterNet can reach 79.41 mAP, and the running speed is 224.224 f/s when the input size is 71 pixel×37 pixel. On the GC61-DET steel plate surface defect dataset, it runs at a speed of 93.10 f/s

up to 31.47 mAP with 512 pixel×512 pixel input size. Huang et al.[18] proposed an auto machine learning (ML) model to detect cylindrical metal surfaces, and the final detection accuracy was 95.5%. It follows that the detection accuracy is around 90% and the large pixel is about 30 f/s.

Theoretically, Zhu and Tian et al.[19] provided a review of the main optical non-destructive testing (NDT) technologies and introduced the history and discussion of recent progress. Then, Yi et al.[20] proposed the eddy current pulse-compression thermography to detect the impact damage and delamination possibly existing in aerospace composite materials. Similarly, Zha et al.[21] completed the detection for groove sizes by using the traditional non-contact visual algorithm, which showed that the absolute error of measurement was 0.031—0.176 mm and the relative error was 0.2%—3.6%. Ma et al.[22] proposed multiobject real-time detection and classification model based on YOLOv3 to detect the traditional advanced ceramic parts, with the mAP reaching 99.19%.

The visual detection object studied in this paper is composite skin part, which has a large external size with complex texture and the characteristics of scattering and reflection on the surface. In this paper, a visual detection method based on deep learning was studied, and a high-precision visual detection system was developed to detect the pits, scratches, mold release cloth marks and fiber tears on the surface of composite skins. It can eliminate the disadvantages of existing methods and improve the accuracy, stability and efficiency of the detection. The main contributions of this paper are listed as follows:

(1) The visual detection system designed in this paper innovatively integrated manipulator module, image acquisition module, laser ranging module, and the deep learning module, which has a high degree of integration and the ability of flexible detection. The upper computer software was designed to precisely control every module to complete specified actions.

(2) For the materials with textured features, the YOLO series of deep learning algorithms were innovatively used to extract and locate defect information. What's more, the dataset for training was expanded for better training effect and finally output detection results in real time.

(3) For parts with radians, a distance adaptive control method of laser ranging sensors and manipulator was proposed to adjust the distance between the cameras and the surface of the part.

1 Visual Detection System Design

Analyses of the shape of aircraft composite skin parts show that the sizes are large with the maximum one reaching 1.4 m × 1.5 m. The parts are not completely flat, which may have different degrees of radian, leading to diverse types and sizes. In order to meet the detection requirements, the design of the detection system in this paper should consider the following aspects:

(1) The size of the detection object is large, therefore the structure of the visual detection units should be simple, compact, reliable, and maintain sufficient rigidity to minimize errors caused by factors such as hardware vibrations.

(2) For parts with radians, the distance adaptive control algorithm is needed to adjust the distance between the cameras and the surface of the part, so as to ensure complete and clear images taken by cameras.

(3) Because of scattering and reflection phenomena on the surface of the parts, multiple sets of cross-examination tests are required for the lighting scheme to ensure that it can achieve the desired effect on the entire surface and highlight the surface feature information.

(4) In order to achieve high detection accuracy and high stability, it is necessary to deeply study image processing algorithms. What's more, high-precision micro-defect recognition algorithms are needed for different types of defects.

(5) The system includes multiple image acquisition units, manipulator motion control units, image processing units, and real-time detection result display units, requiring the multi-threaded, high-

concurrency upper computer software to precisely control hardware modules to complete specified actions.

According to the five points above, this paper proposed a detection scheme based on deep learning. The manipulator was used to grab camera groups to capture surface images of parts, then they were transmitted back to the upper computer for image recognition and the detection results would be displayed. The characteristics of high positioning accuracy and flexibility of the manipulator were used to realize the automatic detection of parts of different models and curvatures, with multiple sets of cameras shooting at the same time to improve the detection efficiency.

In the detection scheme, the hardware modules were divided into manipulator module, image acquisition module, and laser ranging module. The overall layout is shown in Fig.2.

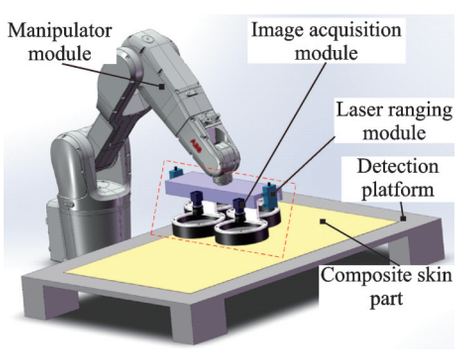

Fig.2 Overall layout of the hardware system

The operation process of the visual detection system for the surface quality of composite skin parts is shown in Fig.3. The operating steps are as follows. (1) Run the manipulator program: Open the upper computer software and turn on the manipulator, and wait for the instructions after running the communication and control program of the manipulator. (2) Lower computer communication: Turn on the laser ranging sensors, and establish socket communication with the manipulator. Then, adjust the parameters of cameras with the light sources on. (3) Place the current detection part: Place the length of the part along the X axis and the width along the Y axis at the origin of the workpiece coordinate system of the detection table. (4) Input part model parameters: Input the part model to be detected in the upper computer software, and the system will compare it with the database to acquire other parameters. (5) Start detection: After starting the detection program, the manipulator moves and carries the cameras shooting according to the calculated path. Then, the upper computer software detects and displays the real-time results of the detection. (6) Completing the detection of the current part, the results are saved to the defect statistics database with the manipulator automatically running to the detection zero point and waiting for the next detection. (7) After the parts are detected, close the upper computer software, and the connection will be automatically broke.

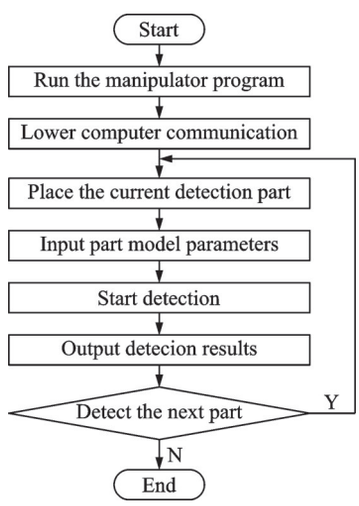

Fig.3 Work flow chart of the detection system

2 Construction of Detection Platform

2.1 Manipulator module

Due to the certain curvature of the composite skin parts, the ordinary three-dimensional motion platform cannot meet the detection requirements. Therefore, the manipulator that could be precisely controlled by the upper computer software was selected as the motion control module, equipped with cameras for shooting.

2.2 Image acquisition module

The industrial camera with 20 million pixels and the resolution of 5 496(H)×3 672(V) was se-

lected, which is small, light and has high reliability. The industrial len with 5 million pixels and the focal length of 8 mm was chose to coordinate with the camera above, then the object distance is calculated to be 114 mm. The depth of field of the cameras and the lens is 16.29 mm, hence the positioning accuracy of the manipulator meets the range limit requirements.

The maximum size of the detected parts can reach 1.4 m × 1.5 m, and the field of view of a single camera is 100 mm × 80 mm. So as shown in Fig. 4, a compact layout of 4 cameras horizontally combined was proposed to reduce the movements of the manipulator and improve the detection efficiency.

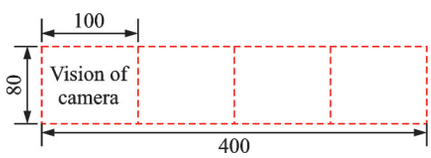

Fig.4 Compact layout

However, the interval between cameras in compact layout is 100 mm. In order to ensure the lighting effect, the outer diameter of the annular low-angle shadowless light source is 180 mm, which cannot be installed. Therefore, a staggered layout was proposed, as shown in Fig.5.

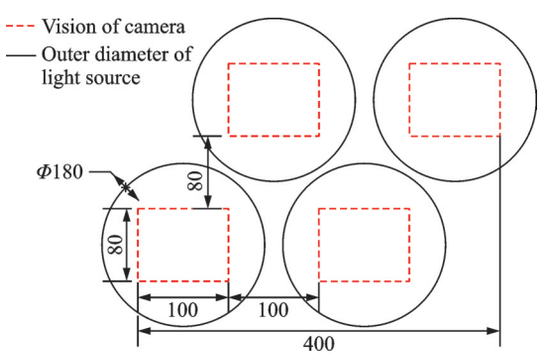

Fig.5 Staggered layout

This staggered layout divides the original row of cameras into two rows with 80 mm row spacing and 100 mm column spacing between cameras. Compared with the compact layout, the staggered layout can ensure the installation space of the annular low-angle shadowless light sources, and the cameras can shoot the entire surface of parts without crossing or omission.

2.3 Laser ranging module

The laser ranging sensor with repeat measurement accuracy of ±1 mm and range of 0.05—40 m was selected to measure the distance between the cameras and the surface of the detected parts.

2.4 Light source

According to the laboratory test results, the surface defects of the detected parts were most clearly displayed under the annular low-angle shadowless light sources, and the uniform illumination could eliminate the interference caused by the uneven surface of parts. After the designs and selections of each module were completed, the components and hardware platform for the surface quality detection of composite materials were assembled, as shown in Fig.6.

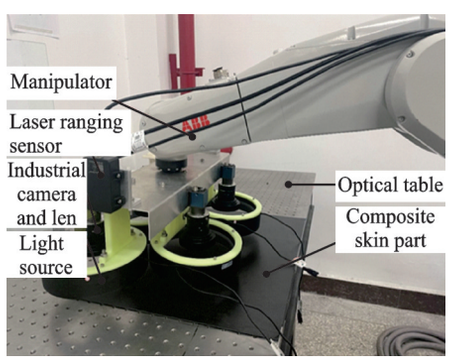

Fig.6 Physical diagram of hardware system

3 Manipulator Motion Control Algorithms

Completing camera calibration and manipulator hand-eye calibration, the top angle of the part to be detected is aligned with the origin of the workpiece coordinate system. After placing the length of the part along the X axis and the width along the Y axis, the number of shots and the movement paths of the manipulator are automatically determined.

For flat composite skin parts, using the manipulator to move at a fixed distance above the part can ensure that the images captured by industrial cameras are within the best imaging range. Thus, there is no need to control the manipulator to adjust the shooting distance between the cameras and the part.

As shown in Fig.7, there is an aircraft compos-

ite skin part selected for detection, whose size is 300 mm × 320 mm. It is part of a large composite skin part, and accordingly the shooting height of the cameras needs to be adjusted to capture high-quality surface images.

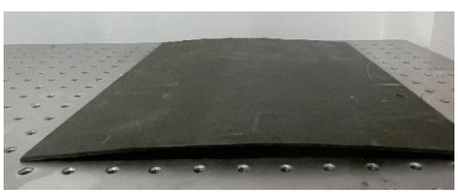

Fig.7 Surface composite skin part with curvature

For composite skin parts with curvature, if the same manipulator movement method is used as for flat parts, the shooting distance may be outside the best imaging range when the cameras move to the highest or lowest point of the cambered surface. Therefore, this paper proposed a distance adaptive control method of laser ranging sensors and manipulator. The laser ranging sensors were installed on both ends of the expansion board of the manipulator end effector, and the posture of the manipulator is adjusted by the distance value returned by the sensors to achieve the acquisition of high-quality images.

The mathematical model of the distance adaptive control method for detected parts with radians is shown in Fig.8, where L is the distance between the two laser ranging sensors; d_i the measured values of laser ranging sensor, $i=1, 2$; d the standard distance between cameras and the parts; R the radius of curvature of the part.

The depth of field of cameras is 16.29 mm, which guarantes the sharpness of shooting within a certain range. In order to simplify the calculation, we only adjusted the angle around Y axis of the manipulator end effector, and the translation adjustments along X axis and Z axis remain the same, which are called θ_Y, ΔX, ΔZ, respectively.

The calculation of θ_Y is

$$\theta_Y = \arctan\frac{d_1 - d_2}{L} \tag{1}$$

where the range of θ_Y is $[-\pi/2, \pi/2]$.

The calculations of ΔX and ΔZ are

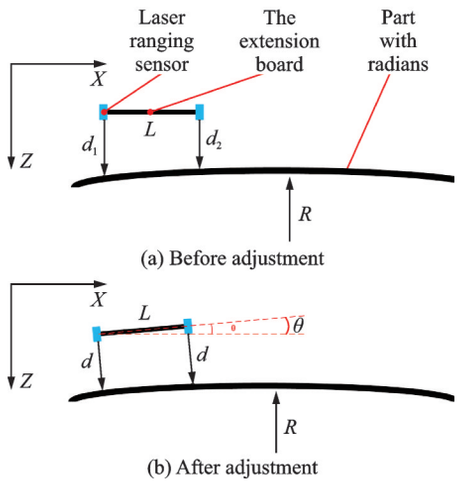

Fig.8 Mathematical model of manipulator adaptive adjustment

$$\begin{cases} \Delta X = -d\sin\theta_Y \\ \Delta Z = d\cos\theta_Y - \dfrac{d_1 + d_2}{2} \end{cases} \tag{2}$$

Every time the manipulator moves to a new detection point, the distance adaptive adjustment is performed according to Eqs.(1, 2) to ensure the clarity of the shooting.

4 Surface Defect Detection of Composite Materials Based on YOLO

4.1 YOLO network

The full name of YOLO is you only look once, and its author Joseph Redmon has released three versions of YOLO: YOLOv1[23], YOLOv2[24], YOLOv3[25]. The core idea of YOLO is to directly output the BBox location information and category information through the neural network of the entire image. YOLO will divide the picture into $S \times S$ grid cells. If the real defect target center is in a certain cell, this cell is responsible for detecting the defect.

4.2 Experiment of YOLOv3 algorithm

YOLOv3 was proposed in 2018, mainly for small target detection, which has good robustness. With multiple independent logistic classifiers for classifications and Darknet-53 being its basic network, it clusters nine anchor boxes, and predicts three BBoxes for each scale, whose advantages are high performance, low background false detection rate, and strong versatility. The algorithm framework of YOLOv3 is shown in Fig.9.

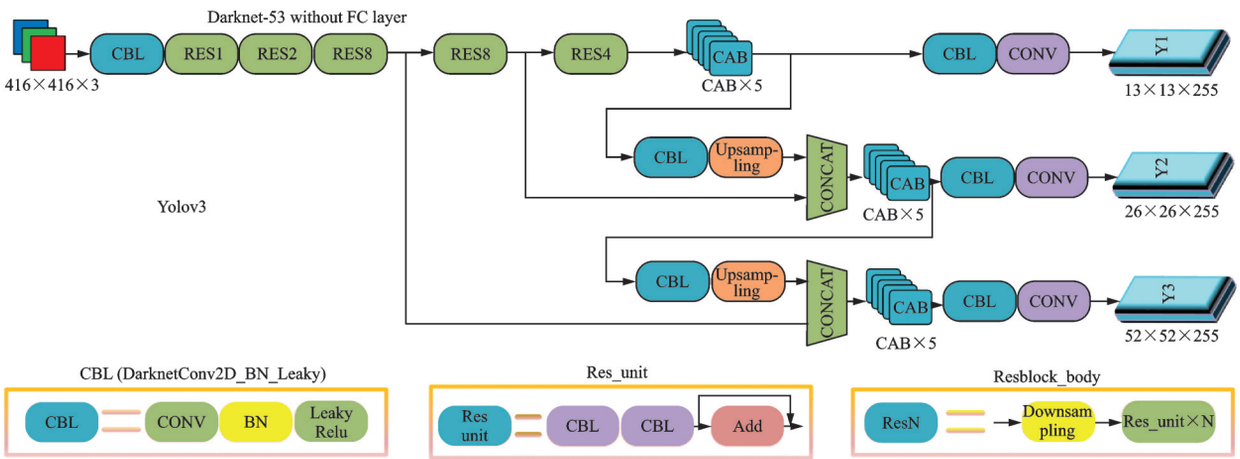

Fig.9 Frames of YOLOv3 algorithm

First of all, it is necessary to establish sample images of the surface defects of the parts. In actual manufacture process, the probabilities of defects on the surface of the part are very small, leading to not enough defects obtained for training. Therefore, we need to expand the surface defect dataset with data augmentation. Expanding the dataset has the following two functions:

(1) Increase the number of surface defect samples and improve the accuracy of model detection.

(2) Resist noise interference at the detection sites and maintain the stability of detection.

By using the following three dataset expansion methods: Mirroring and rotating, translating, and adding noise, we obtained a total of 1 851 images with the size of 512 pixel × 512 pixel. After that, with the deep learning dataset labeling tool named LabelImg, we used rectangular boxes to select the defects and label the types. Finally, the labeled dataset was scrambled and sent to the model for learning in random order. The number of iterations was 300, and the dataset was divided into training set and test set according to the ratio of 9∶1.

For most defects, the detection results were good and the confidence was high. However, by studying the prediction results of the test dataset, it was found that there were still some problems with the training weights of YOLOv3:

(1) For samples with a large proportion of defects in the image, the detection confidence was low. As shown in Figs.10(a, b), the scratch area accounts for 45% and 40% of the image proportion, and the confidence level is only 0.29 and 0.53, respectively. By analyzing the detection results of the test set, the larger the proportion of defects in the image is , the lower the confidence is.

(2) The detection confidence is low for the inconspicuous mold release cloth marks. As shown in Figs.10(c,d), the confidence levels of the mold release cloth marks here are only 0.30 and 0.20, respectively. Compared with the traditional algorithms, the deep learning algorithm has been able to detect the defects here, but it is still necessary to make appropriate adjustments to improve the detection confidence.

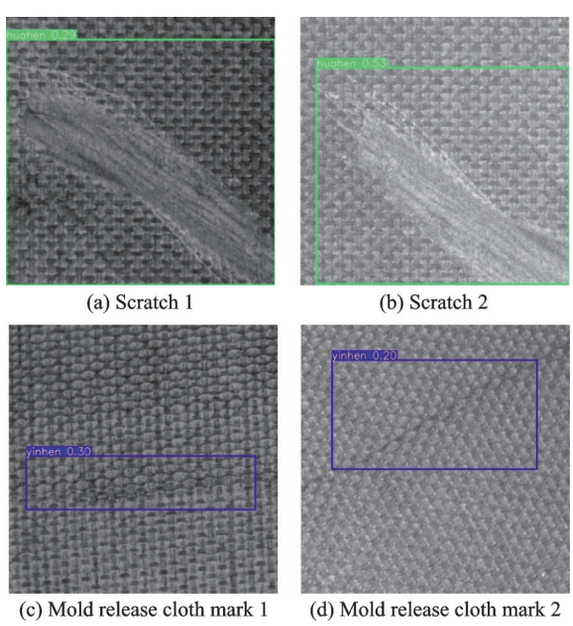

(a) Scratch 1 (b) Scratch 2

(c) Mold release cloth mark 1 (d) Mold release cloth mark 2

Fig.10 Problems in detect results

4.3 Improved test based on YOLOv5

The experimental results of the YOLOv3 training model have many shortcomings. Therefore, the dataset and model were adjusted to achieve better detection effects.

The YOLOv5 network is the latest network of the YOLO architecture series. It was proposed by Ultralytics in May 2020, whose fastest detection speed can reach 140 f/s with the advantages of high detection accuracy and strong real-time performance. At the same time, the weight file size of YOLOv5 network model is nearly 90% smaller than that of YOLOv4 published by Alexey Bochkovskiy in April, so it is very suitable for being deployed on embedded devices for real-time detection. Different from YOLOv3, YOLOv5 abandons the main structure of Darknet-53 and uses BackBone as the main network, which is mainly responsible for abstracting the input images into features. Its model structure is shown in Fig.11.

In Section 4.2, 1 851 images with size of 512 pixel×512 pixel were produced by means of the augmented dataset. However, through the analysis and detection results, it was found that the size of some defects was too large, which led to that the images of 512 pixel × 512 pixel could only display part of scratches or mold release cloth marks. Therefore, referring to the method of making dataset in Section 4.2, the surface defects were reintegrated and expanded, and a new dataset was made. The comparison between the new dataset and the original dataset is shown in Table 1.

Table 1 Comparison between new and original dataset

Parameter	Original dataset	New dataset
Image size/(pixel×pixel)	512×512	1 024×1 024
Pit/sheet	25	649
Scratch/sheet	759	1 010
Mold release cloth mark/sheet	1 037	2 848
Fiber tearing/sheet	30	579
Sum/sheet	1 851	5 086

By setting the same parameters and using the deep learning models of YOLOv3 and YOLOv5 to train the original dataset and the new dataset, respectively, we could compare the results in terms of defect detection difference.

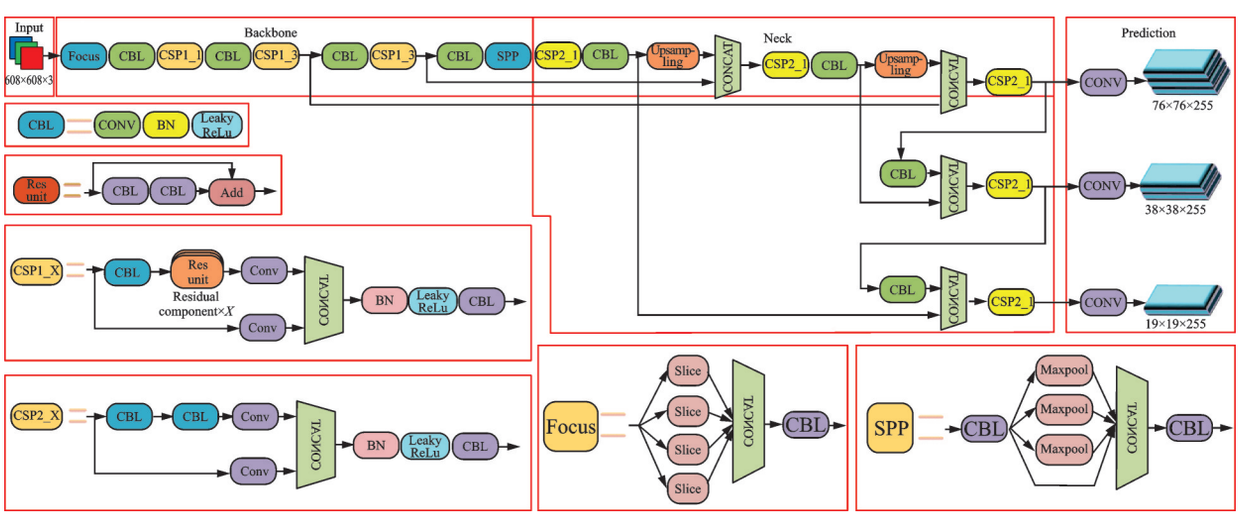

Fig.11 Model structure of YOLOv5

4.3.1 Training efficiency

For the training of YOLOv3 and YOLOv5 models, the same training parameters were used: The number of training iterations (epochs) is 500, while the number of samples for one training (batch_size) is 4, and the training time is shown in Table 2.

Table 2 Comparison of training time

Algorithm	Original dataset/h	New dataset/h
YOLOv3	3.7	5.9
YOLOv5	2.1	4.1

As can be seen from Table 2, because the new dataset is superior to the original dataset in terms of image sizes and image richness, the training time is longer. Comparing the training time of YOLOv5 and YOLOv3, it can be seen that the training efficiency of YOLOv5 has more advantages.

4.3.2 Training accuracy

The precision-recall (PR) curve and mAP are used to evaluate the effect of training. TP, TN, FP and FN are the abbreviations of true positive, true negative, false positive, and false negative, respectively. Positive and negative indicate the result obtained by the prediction. True and false indicate whether the predicted result is the same as the real one.

The formula for calculating the accuracy rate is shown below, indicating the percentage of correctly identified samples in all identified samples.

$$\text{Precision} = \frac{\text{TP}}{\text{TP} + \text{FP}} \tag{3}$$

The formula for calculating the recall rate is shown below, indicating the percentage of correctly identified samples in all samples.

$$\text{Recall} = \frac{\text{TP}}{\text{TP} + \text{FN}} \tag{4}$$

The PR curve is shown in Fig.12, where Fig.12(a) is the training PR curve of the original dataset, and Fig.12(b) the training PR curve of the new dataset. As can be seen from the figure above, the PR curve in Fig.12(b) can completely wrap that in Fig.12(a), so the training effect of the new dataset is better than that of the original one.

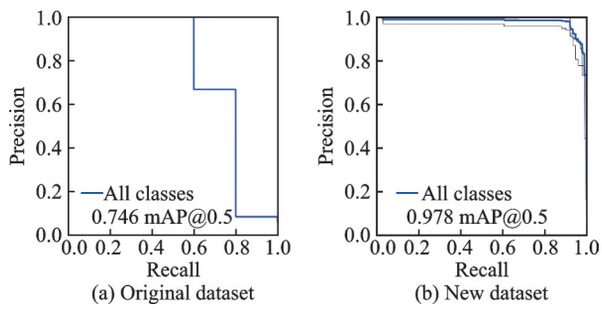

Fig.12 PR graphs

5 Analysis of Detection Results

5.1 Comparison of different algorithms

In order to demonstrate the superiority of the YOLOv5 detection algorithm, it was compared with the traditional visual processing algorithm and the YOLOv3 algorithm. The results are shown in Table 3.

Table 3 Comparison of detect results %

Algorithm	AP				mAP
	Pit	Scratch	Mold release cloth mark	Fiber tearing	
Traditional visual processing algorithm	72.32	50.16	46.96	48.29	54.43
YOLOv3	83.26	74.38	71.45	84.79	78.47
YOLOv5	94.29	100	93.75	96.43	96.35

Experimental results show that the YOLOv5 detection algorithm used in this paper has good performance: The detection accuracy is better than that of other detection algorithms and the detection effect of each type of defect is relatively average.

5.2 Detect efficiency of YOLOv5

The YOLOv5 model was used to train the original dataset and the new one, respectively. Then, the two weights obtained from the training were used to detect the defect sample images of the corresponding size. By comparing the detection efficiency, the average detection time and detect efficiency of the two weight files are shown in Table 4.

Table 4 Comparison of detect time and detect efficiency

Image size/ (pixel×pixel)	Detect time/s	Detect efficiency/ ($f \cdot s^{-1}$)
512×512	0.017	58
1 024×1 024	0.031	32

The size of the original image captured by industrial cameras is 5 496 pixel×3 672 pixel, which is used as the standard image format to analyze the detection efficiency of the model. After the image is split, the slider-type detection is performed. When

the cell size is 512 pixel×512 pixel, each image needs to be detected 88 times, and it takes 1.496 s to detect a standard image. When the cell size is 1 024 pixel×1 024 pixel, the detect times of each image is 24, and a standard image takes 0.744 s. It can be seen that the detection model trained by the new dataset has a large image size and a long single detection time, but the complete detection of a standard image is more efficient, which is about twice as high as that of the original dataset.

5.3 Detect accuracy of YOLOv5

In order to verify the detection accuracy of the surface quality detection system for composite skin parts designed in this paper, and to verify the generalization performance of the deep learning model at the same time, new defects were created for the laboratory part samples. For the mold release cloth marks that caused by improper operation in the manufacture process and cannot be replicated, the samples that have not been used for training were selected as the validation set. A total of 137 new defects were selected to be shooted and detected by the software system, and the detect results were analyzed.

The typical defect detection results are shown in Fig.13, and the total results are shown in Table 5. In Table 5, the defect number are the actual number of four types of defects: Pits, scratches, mold release cloth marks, and fiber tearings. The total number of samples whose detection result categories are consistent with the real categories and whose confidence level is higher than 60% are defined as correct detections. Those whose detection result categories are inconsistent with the real categories are considered as misdetections. Defects that are not detected are regarded as missed detections.

The accuracy rate was used to evaluate the detect results which refered to the ratio of the number of targets accurately detected to the total number of verification datasets. The accuracy rate of the detection is 96.35%, which meets the accuracy requirement for the detection of composite skin parts. Among the misdetected defects, a fiber tearing was mistakenly identified as a scratch. These two de-

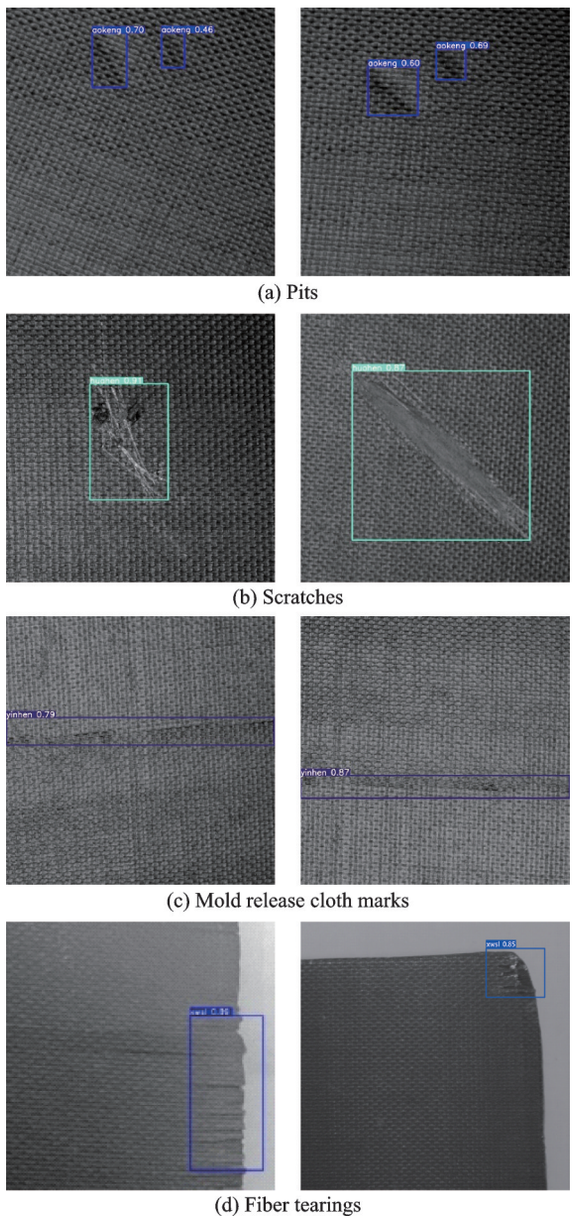

(a) Pits

(b) Scratches

(c) Mold release cloth marks

(d) Fiber tearings

Fig.13 Typical defects of composite skin parts

Table 5 Detect results

Parameter	Pit	Scratch	Mold release cloth mark	Fiber tearing	Sum
Defects number/sheet	35	42	32	28	137
Correct detection/sheet	33	42	30	27	132
Misdetection/sheet	0	0	0	1	1
Missed detection/sheet	2	0	2	0	4

fects have a certain degree of similarity at a specific angle, while fiber tearings mostly occur at the edge of the surface of the part and scratches mostly appear in the center. Among the missed identification defects, two cases of pits and two cases of mold release cloth narks were missed. Such defects have stricter lighting requirements, so the missed detection rate is higher than that of the other.

6 Conclusions

In addition to the high efficiency of non-contact detection, the novelty of the detection method proposed in this paper is rapidity, flexibility, and accuracy. It takes 0.744 s to complete detection of an image with a size of 5 496 pixel × 3 672 pixel, with the detection accuracy reaching 96.35%. And it can detect composite skin parts with different curvatures.

Based on the carried out studies, we obtain the following conclusions.

(1) According to the detection scheme, the detection platform was built. In order to improve the detection efficiency, the manipulator was equipped with four sets of industrial cameras and light sources to capture the surface images of the composite materials, and the laser ranging sensors and the manipulator were used to detect the curved surface of the composite material skin parts.

(2) The complementary upper computer software was developed at the same time. During the detection process, the detection information could be displayed in real time on the upper computer, and finally saved into the database.

(3) Due to the lack of raw composite skin parts, the dataset for YOLOv5 network was expanded by employing the following three methods: Mirroring and rotating, translating, and adding noise.

(4) The YOLOv5 deep learning method was used in this paper, with the mAP reaching 0.978 when the IOU threshold is 0.5, and the detection efficiency reaches 32 f/s. Thus, the plantform meets the requirements of composite surface quality detection and can be applied to the detection of actual composite skin parts.

As for the future work, the detection system can be improved in the following aspects.

(1) Further improve the adaptive distance control algorithm: The composite skin parts can be modeled in 3D modeling software, and the manipulator can be controlled more precisely through the analysis of the model. Particularly, the special-shaped composite parts with more complex shapes can be detected with high efficiency and accuracy.

(2) Further improve the accuracy of the defects detection: Other target detection algorithms can be tested to further improve the accuracy of the system, such as region-CNN (R_CNN), single shot multiBox detector, etc. What's more, the existing algorithms can be modified to make it more suitable for the detection of composite skin parts.

References

[1] SIEGEL M, GUNATILAKE P. Remote inspection technologies for aircraft skin inspection[C]//Proceedings of IEEE Workshop on Emergent Technologies and Virtual System for Instrumentation and Measurement. [S.l.]: IEEE, 1997: 69-78.

[2] SIEGEL M, GUNNATILAKE P, PODNAR G. Robotic assistance for aircraft inspectors[J]. Industrial Robot, 1998, 25(6): 389-400.

[3] SIEGEL M, KAUFMAN W M, ALBERTS C J. Mobile robots for difficult measurements in difficult environments: Application to aging aircraft inspection[J]. Robotics and Autonomous Systems, 1993, 11(3/4): 187-194.

[4] BACKES P G, BAR-COHEN Y, JOFFE B. The multifunction automated crawling system[C]//Proceedings of IEEE International Conference on Robotics & Automation. [S.l.]: IEEE, 1997, 1: 335-340.

[5] WHITE T S, ALEXANDER R, CALLOW G, et al. A mobile climbing robot for high precision manufacture and inspection of aerostructures[J]. The International Journal of Robotics Research, 2005, 24(7): 589-598.

[6] SHENG Min. Aircraft skin damage detection method based on machine vision[D]. Nanjing: Nanjing University of Aeronautics and Astronautics, 2013. (in Chinese)

[7] LIU Hengxin. Damage detection and recognition of aircraft surface image using deep network[D]. Beijing:

Beijing University of Posts and Telecommunications, 2018. (in Chinese)

[8] YAN Zhanxiao. Infrared image recognition of damage in the airplane skin based on machine learning[D]. Tianjin: Civil Aviation University of China, 2017. (in Chinese)

[9] VIOLA P, JONES M J. Robust real-time face detection[J]. International Journal of Computer Vision, 2004, 57(2): 137-154.

[10] VEDALDI A, GULSHAN V, VARMA M, et al. Multiple kernels for object detection[C]//Proceedings of 2009 IEEE 12th International Conference on Computer Vision. [S.l.]: IEEE, 2009: 606-613.

[11] HARZALLAH H, JURIE F, SCHMID C. Combining efficient object localization and image classification[C]//Proceedings of 2009 IEEE 12th International Conference on Computer Vision. [S.l.]: IEEE, 2009: 237-244.

[12] KUANG H L, CHAN L L H, YAN H. Multi-class fruit detection based on multiple color channels[C]//Proceedings of 2015 International Conference on Wavelet Analysis and Pattern Recognition (ICWAPR). [S.l.]: IEEE, 2015: 1-7.

[13] LOWE D G. Distinctive image features from scale-invariant keypoints[J]. International Journal of Computer Vision, 2004, 60(2): 91-110.

[14] LIENHART R, MAYDT J. An extended set of HAAR-like features for rapid object detection[C]//Proceedings of International Conference on Image Processing. [S.l.]: IEEE, 2002.

[15] SERMANET P, EIGEN D, ZHANG X, et al. OverFeat: Integrated recognition, localization and detection using convolutional networks[J]. Computer Vision and Pattern Recognition, 2014. DOI: 10.48550/arXiv.1312.6229.

[16] GIRSHICK R, DONAHUE J, DARRELL T, et al. Rich feature hierarchies for accurate object detection and semantic segmentation[C]//Proceedings of the IEEE Conference on Computer Vision and Pattern Recognition. [S.l.]: IEEE, 2014: 580-587.

[17] HE K, ZHANG X, REN S, et al. Spatial pyramid pooling in deep convolutional networks for visual recognition[J]. IEEE Transactions on Pattern Analysis and Machine Intelligence, 2015, 37(9): 1904-1916.

[18] GIRSHICK R. Fast R-CNN[C]//Proceedings of the IEEE International Conference on Computer Vision. [S.l.]: IEEE, 2015: 1440-1448.

[19] LIU Yajiao, YU Haitao, WANG Jiang, et al. Surface detection algorithm of multi-shape small defects for section steel based on deep learning[J]. Journal of Computer Applications, 2022, 42(8): 2601-2608.

[20] TIAN R, JIA M. DCC-CenterNet: A rapid detection method for steel surface defects[J]. Measurement, 2022, 187: 110211.

[21] HUANG Y C, HUNG K C, LIN J C. Automated machine learning system for defect detection on cylindrical metal surfaces[J]. Sensors, 2022, 22(24): 9783.

[22] ZHU Y K, TIAN G Y, LU R S, et al. A review of optical NDT technologies[J]. Sensors, 2011, 11(8): 7773-7798.

[23] YI Q, TIAN G Y, MALEKMOHAMMADI H, et al. New features for delamination depth evaluation in carbon fiber reinforced plastic materials using eddy current pulse-compression thermography[J]. Ndt & E International, 2019, 102: 264-273.

[24] ZHA Anfei, LU Yonghua, WANG Mingxin, et al. Research on visual detection algorithm for groove feature sizes by means of structured light projection[J]. Transactions of Nanjing University of Aeronautics & Astronautics, 2022, 39(3): 367-378.

[25] MA Chenkai, WU Yihui, FU Huaqi, et al. Real-time defect detection system for advanced ceramic parts based on deep learning[J]. Journal of Nanjing University of Aeronautics and Astronautics, 2021, 53(5): 726-734. (in Chinese)

[26] REDMON J, DIVVALA S, GIRSHICK R, et al. You only look once: Unified, real-time object detection[C]//Proceedings of the IEEE Conference on Computer Vision and Pattern Recognition. [S.l.]: IEEE, 2016: 779-788.

[27] REDMON J, FARHADI A. YOLO9000: Better, faster, stronger[C]//Proceedings of the IEEE Conference on Computer Vision and Pattern Recognition. [S.l.]: IEEE, 2017: 7263-7271.

[28] REDMON J, FARHADI A. YOLOV3: An incremental improvement[EB/OL]. (2018-04-08). https://arxiv.org/pdf/1804.02767.pdf.

Acknowledgements This work was supported by the National Natural Science Foundation of China (No. 51975293) and the Aeronautical Science Foundation of China (No. 2019ZD052010).

Author Prof. LU **Yonghua** received his Ph. D. degree from Nanjing University of Aeronautics and Astronautics in 2005. He is currently a professor at Nanjing University of

Aeronautics and Astronautics. His main research interests include intelligent measurement and control, measurement system and robotics.

Author contributions Prof. **LU Yonghua** provided the theoretical basis and experimental guidance. Mr. **HUANG Yu** designed the study, compiled the models, conducted the analysis, interpreted the results, and wrote the manuscript. Dr. **XU Jiajun** contributed to data and model components for the study. Mr. **FENG Qiang** contributed to the discussion and background of the study. Mr. **ZHOU Lihua** contributed to data for the analysis of the study. All authors commented on the manuscript draft and approved the submission.

Competing interests The authors declare no competing interests.

(Production Editor: XU Chengting)

基于深度学习的复材表面缺陷检测方法

陆永华[1], 黄 钰[1], 徐嘉骏[1], 冯 强[2], 周利华[2]

(1.南京航空航天大学机电学院, 南京 210016, 中国; 2.国营锦江机器厂, 成都 610043, 中国)

摘要: 随着航空航天材料节能减重的发展趋势,高性能复合材料在飞机蒙皮中得到了广泛的应用。然而,对复合材料蒙皮零件的表面质量检测多由人工方式进行,检测效率低,精度低。近年来,视觉检测越来越受到人们的关注,主要是因为它的高精度和高灵活性的无损检测特性。针对复合材料蒙皮零件表面缺陷的视觉检测需求,本文搭建了基于机器人的检测平台,该平台创新性地集成了机械手模块、图像采集模块、激光测距模块、深度学习模块以及配套的上位机软件。为了保证检测的效率和准确性,本系统基于YOLOv5开发了检测算法。此外,由于缺乏原始复合材料蒙皮零件,系统通过镜像旋转、平移和添加噪声3种方法对训练数据集进行扩展。实验证明,该系统能够实现对各类复合材料蒙皮零件的在线、自动化和准确地检测。该系统可以在0.744 s内完成尺寸为5 496像素×3 672像素的图像检测,且检测精度达到96.35%,满足复合材料表面质量检测的要求。

关键词: 复材蒙皮;视觉检测;YOLO;目标检测;机械手